Evaluation of a State-of-the-Art Indoor Mobile Mapping System in a Complex Indoor Environment

Untersuchung eines modernen Indoor Mobile Mapping Systems in komplexen Innenräumen

Cigdem Askar | Annette Scheider | Harald Sternberg

Summary

Nowadays, terrestrial laser scanning (TLS) is a standard industry method for data acquisition in building modelling. However, terrestrial laser scanning in stand-still mode and occlusion posed by the environment make TLS time-consuming. Mobile indoor mapping systems speed up the scanning procedure and handle the occlusion problem. Here, a performance assessment of a state-of-the-art mobile indoor mapping system (NavVis VLX 2) is presented and compared to a terrestrial laser scanner (Z+F Imager 5016) for building documentation in a complex indoor environment. The assessment focuses on the representation of geometry of the scanned environment. The results show that the mobile mapping system NavVis VLX 2 is promising in these surroundings, with accuracies up to 2.5 cm and a low noise level.

Keywords: indoor mobile mapping systems, 3D Scanning, point cloud comparison

Zusammenfassung

Heutzutage stellt terrestrisches Laserscanning (TLS) eine Standardmethode zur Datenerfassung bei der Gebäudemodellierung dar. Das Scannen mit Stativ und die dabei teilweise auftretende Abschattung durch umgebende Strukturen machen das terrestrische Laserscanning jedoch sehr zeitaufwändig. Mobile Indoor-Mapping-Systeme beschleunigen den Scanvorgang und lösen meist das Problem mit Abschattungen. Hier wird die Leistungsfähigkeit eines modernen mobilen Indoor-Mapping-Systems (NavVis VLX) im Vergleich zu einem terrestrischen Laserscanner (Z+F Imager 5016) zur Gebäudedokumentation in einer komplexen Innenraumumgebung bewertet. Der Schwerpunkt der Untersuchung liegt auf der Darstellung der Geometrie der gescannten Umgebung. Die Ergebnisse zeigen, dass das NavVis VLX Mobile Mapping System in dieser Umgebung mit einer Genauigkeit von besser als 2,5 cm und einem geringen Rauschen vielversprechend ist.

Schlüsselwörter: *Indoor-Mobile-Mapping-System, 3D Scanning, Punktwolkenvergleich*

1 Introduction

In the context of Industry 4.0, digitalization and artificial intelligence cause a change in the conventional industry's labour-intensive practices in the Architecture, Engineering and Construction (AEC) industry (Wu et al. 2022). In this regard, building information modelling (BIM) gained more attention as it brings digitalization and artificial intelligence into the AEC industry. BIM can be defined as a knowledge repository that generates and maintains building information throughout a facility's life cycle (Wang et al. 2019). Widespread use cases of BIM include documenting the design and as-built representations, documentation of changes, early detection of clashes, depicting consistent vertical and horizontal sections, effective cost-estimations, analysis and simulations on the asset for facility management purposes (Borrmann et al. 2018). 3D Scanning is, therefore, highly integrated into the BIM workflows (Scan-2BIM), especially in the as-built and change documentation. Hence, the quality of the point cloud is critical for successful modelling processes. Generally, the requirements for the geometric quality of a project are defined according to the Level of Accuracy (LOA) specifications, which are established through the use of the standard deviation, a well-known concept in geodesy. LOA specifications are formed by five levels and are defined by the increments of tens attached to LOA (e. g. LOA10, LOA50), corresponding also with the classifications outlined in the German standard DIN 18710-1 (DIN 2010, Becker et al. 2022). The lowest level is LOA10, which allows a maximum deviation of 5 cm accuracy, while the highest level is LOA50, which demands accuracies up to 1 mm (Tab. 1). The chosen accuracy level has to be described in the project document

Tab. 1: LOA Levels defined by the U. S. Institute of Building Documentation. The table numbers are determined based on the deviation of 2σ. (U. S. Institute of Building Documentation 2016)

Level	Upper Range	Lower Range
LOA10	User-defined	5 cm
LOA20	5 cm	15 mm
LOA30	15 mm	5 mm
LOA40	5 mm	1 mm
LOA50	1 mm	0

  DOI 10.12902/zfv-0445-2023

either as measured accuracy, which is meant to assess the measurements (e. g., point cloud accuracy) or as represented accuracy, which evaluates the measured data processed into another format, such as a mesh model generated from the point clouds (U. S. Institute of Building Documentation 2016).

The data capture in 3D scanning is demonstrated statically or kinematically. Terrestrial laser scanners are often used in a static data acquisition mode that provides very high-qualitative point clouds (Soudarissanane 2016). Its disadvantage is the occlusion in interiors, which needs multiple setups to overcome (Janßen et al. 2022). On the other hand, the kinematic approach has been favoured in recent years owing to its ease of use and speed and has been widely used in outdoor scenes, such as the acquisition of road applications (Heinz et al. 2020). In this case, the indoor mapping system is mobile and performs scanning while moving through the rooms, and this movement reduces the occlusion problem. In the absence of GNSS signals in interiors, the localization issue in the kinematic systems is resolved mainly through utilizing the Simultaneous Localisation and Mapping (SLAM) technique (Salgues et al. 2020). In this technique, the scanner's position is determined with the fusion of data from the system's sensors, e. g., IMU, lidar and camera, during the scanning process (Higgins 2020a). Although not as popular, other solutions are based on external localization, e. g., in Keller (2016). There are different solutions to mount a mobile indoor mapping system: handheld, trolley, and backpack constellations (Otero et al. 2020). The handling of each constellation differs based on the platform's mobility. Handheld scanners are the smallest solution, which are easy to use and particularly advantageous for spaces that are small and difficult to reach. Systems mounted on trolleys can be loaded with heavier sensors, thus providing better qualities; however, they are limited to flat surfaces (Lehtola et al. 2017). Wearable solutions are comfortable to carry and can achieve good quality, but it might be challenging to capture some spaces. As the interest in mobile indoor mapping systems gradually grew in recent years, more studies were published assessing different mobile mapping systems. Lehtola et al. (2017) compared five commercial indoor mapping systems and three research prototypes against survey-grade TLS point clouds from various test sites with distinct properties. Based on the authors' proposed comparison, among different mounting configurations, wheeled platforms, FGI Slammer and NavVis M6, provided the most precision, although they were restricted to mainly flat surfaces. Maboudi et al. (2017) investigated the trolley-based system Viametris iMS3D and the handheld scanner GeoSLAM Zero-Revo in a controlled environment compared to the survey-grade scanner Leica P20. The results offered a reasonable standard deviation of around 10 mm for both systems. Tucci et al. (2018) examined three indoor mobile mapping systems (Kaarta Stencil, Pegasus Leica Backpack and GeoSlam Zeb-Revo) and presented the RMS of distances, with respect to the ground truth, as 4 to 8 cm. Salgues et al. (2020) evaluated two mobile mapping systems (handheld GeoSLAM ZEB-Revo RT and backpacked GreenValley LiBack C50) for indoor surveys. The evaluation used a TLS point cloud as reference data, and both mobile systems provided similar results with a reachable accuracy of 1 cm, defined as very satisfying and promising by the authors.

This paper will assess the NavVis VLX 2, a state-of-the-art wearable mobile indoor mapping system, compared to a survey-grade scanner Z+F Imager 5016 in a complex building environment. The test environment has thick concrete walls lacking texture and sometimes with sharp edges. Also, extensive glass features, one side wall of a hallway and big windows make up a significant portion of the test floor, along with the narrow, long, sloped spaces. These properties are common problem sources for laser scanning in indoor spaces (Lehtola et al. 2021). Hence, this paper focuses on the performance assessment on a complex building floor in the context of building documentation within the indoor navigation project "Level 5 Indoor Navigation" (Schuldt et al. 2021). In this regard, the correctness and accuracy of point clouds will be investigated, as well as the noise measurements through primitive fittings. Finally, the results will be discussed in relation to the LOA specification (Tab. 1).

2 Investigated Systems and Data Capture

The investigated system, NavVis VLX 2 (Fig. 1), is categorized as a wearable mobile indoor mapping system. It consists of two multi-layer Velodyne VLP-16 lidar

NavVis 2023

Fig. 1: NavVis VLX

sensors (Higgins 2020b) for scanning and localization simultaneously. In addition, four cameras are positioned on top of the instrument to take pictures automatically or manually. At the beginning of each scanning session, the instrument calibrates itself with a short initialization process. For that purpose, it is laid on the ground and turned 90 degrees left and right. As NavVis VLX captures data while moving, it uses SLAM algorithms to determine its trajectory. Therefore, trajectory errors and drift are possible over time (Prokhorov et al. 2019). To improve the trajectory localization and, if needed, for georeferencing, survey markers are placed and used as control points at a distance of 25 to 30 m on the walls or the ground of the scanned area. The relative accuracy of the point cloud (without control points) is 8 mm in 1σ (measured in a room of 100 m²) and depends on the environment (NavVis 2020). A Summary of NavVis VLX's specifications is given in Tab. 2.

The survey area covers two floors (ground and first floor) of the HafenCity University building in Hamburg. In this comparison test, mainly the first floor's data is used (Fig. 3). Long narrow hallways, slanted grounds, complete glass walls, open spaces, stairs and building components like columns are characteristics of this test site.

The NavVis VLX 2 data was captured in September 2021 through the Hamburg-based company DiConneX on the HafenCity University test floors. The data (Fig. 2) was delivered in *.rcp and *.e57 formats after DiConneX completed post-processing, and it is assumed that it is the best output data from the system. One person completed the scanning in one hour, and the delivered point cloud had around 90 million points. Six control points were used to improve the localization, and the trajectory consists of multiple closed loops to eliminate drift errors. Besides, other geodetic control points, which were already placed on the floors and

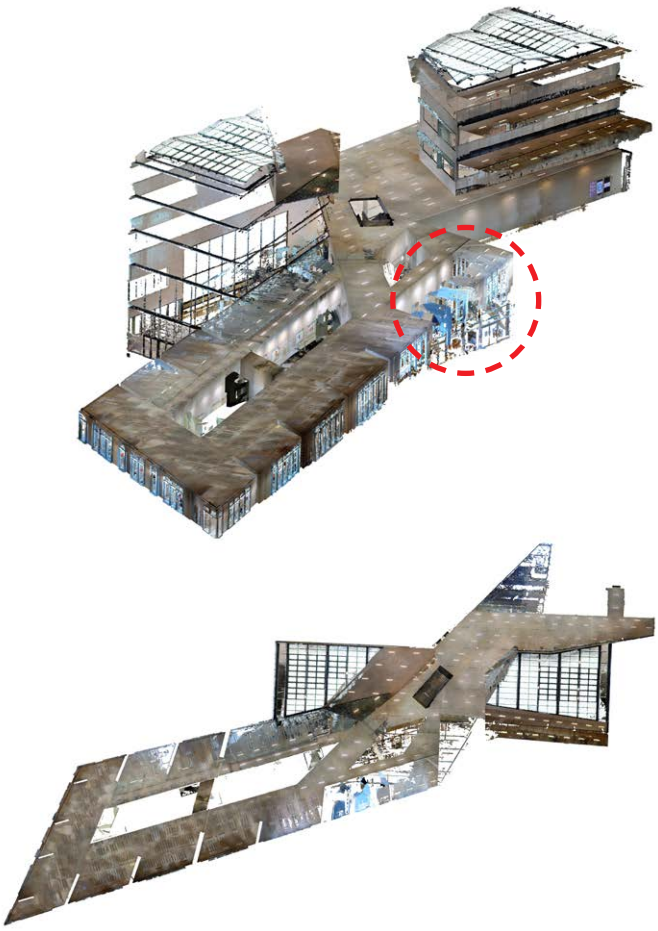

Fig. 2: Post-processed point cloud from the NavVis VLX. The post-processing algorithm detects and cleans the noise behind glass surfaces bordering the outside. However, inside, it does not detect the noise, e.g., in the area inside the red circle, where noise behind the glass wall of the hallway is not cleaned.

Tab. 2: Technical specifications of the NavVis VLX and Z+F Imager 5016 (NavVis 2020, Zoller + Fröhlich, n.d.)

	NavVis VLX	Z+F Imager 5016 (reference system)
Dimensions (H × W × L)	108 × 33 × 56 cm	32.8 × 15 × 25.8 cm
Weight	9.3 kg	6.8 kg
Battery	2 × 2 Li-on V-Mount Micro, hot-swappable	2 batteries (+2 additional), hot-swappable
Sensors	IMU, Bluetooth, Wifi (for data transfer)	IMU, GPS, Dynamic compensator, Wifi (for data transfer)
Number of laser scanners	2 × 16-layer	1
Wavelength	903 nm	1500 nm
Field of View (FOV)	360° horizontal, 360° vertical	360° horizontal, 320° vertical
Range	max. 100 m	up to 365 m
Points per second	2 × 300,000	max. 1.1 million
Number of cameras	4	1
Image resolution	4 × 20 megapixel	80 megapixel
Lens	Fisheye, 3.3 mm, aperture f/2.4	HDR camera
Relative accuracy	8 mm (1σ, measured in a room of 100 m²)	≤ 1 mm + 10 ppm/m (linearity)
Output formats	E57, LAS, PTS, XYZ, PLY	E57, ASC, PTS, RCP, ZFS etc.

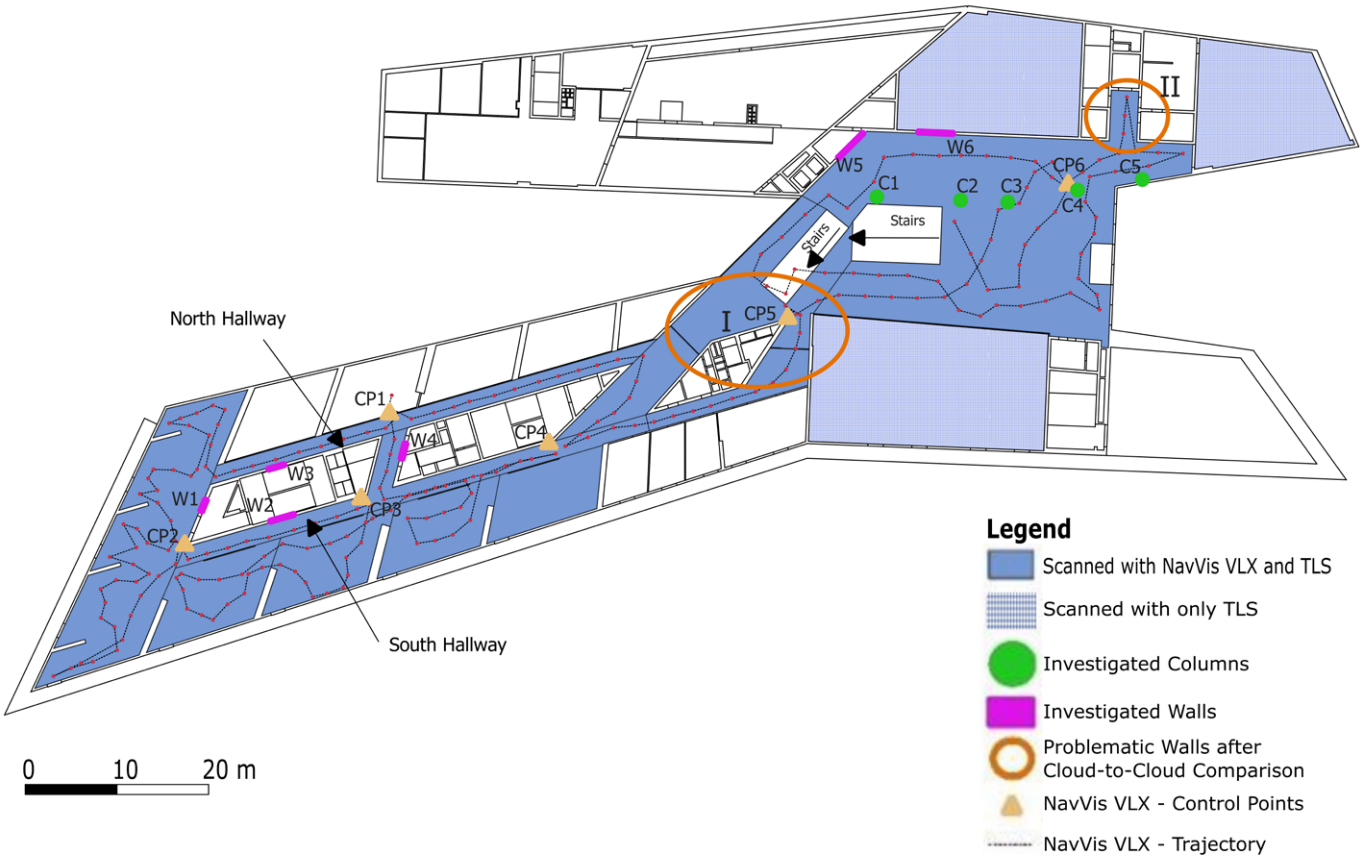

Fig. 3: Floor plan of the test field, showing scanned spaces, evaluates structures (Wall and Columns), control points (CP), and NavVis VLX trajectory

measured by a total station, were scanned to georeference the final point cloud so that both point clouds are in a common coordinate system. Reference data was captured by Z+F Imager 5016 in March to April 2021. Eighty-one scan stations (70 of which cover the NavVis VLX 2 captured spaces) were used to capture the first floor (Fig. 4). One operator worked for two days to finish the work, including placing paper targets on the site. Data was registered, processed and filtered in the manufacturer's software, Z+F Laser Control. A subsampled point cloud was exported in *.e57 format with around 118 million points. Z+F Imager 5016 is a compact and state-of-the-art terrestrial laser scanner by Zoller+Fröhlich (Germany). It can measure more than one million points per second in the range of up to 360 m and offers up to 0.1 mm range resolution (Zoller + Fröhlich, n. d.). However, this data set's resolution in the 10 m range was chosen as 6.3 mm. Tab. 2 depicts the technical specifications of the Z+F Imager 5016. Hereafter, Z+F Imager 5016 will be referred to as TLS.

3 Data Processing and Comparison Methodology

As the authors had been delivered with the post-processed NavVis VLX data, they have brief information about the post-processing procedure. Captured data goes through an automatic post-processing step in the manufacturer's software, *NavVis Sitemaker*, that works only in Ubuntu or Linux operating systems. User interaction in the software is limited, with an important setting being the resolution (distance between two points), set to 10 mm for this study. Optionally, users can input geodetic control point coordinates and select panorama pictures. After post-processing, point clouds can be exported in the desired format or further processed in a web processing step (not relevant for this work), generating a tiled point cloud with panorama pictures and publishing in NavVis' web viewer. The authors shared control point coordinates with DiConneX to obtain georeferenced point clouds. A preliminary check was conducted on the received NavVis VLX point cloud in comparison to the delivered control point coordinates, and the root-mean-square-error (RMSE) for X, Y, and Z coordinates was calculated to be 1 cm.

The reference data from Z+F Imager 5016 (Fig. 4) was first filtered, e. g., considering mixed pixels, single pixel and intensity filters, and cleaned to remove data captured behind the glass objects. After filtering and cleaning, due to the challenging structure of the building with featureless walls, the point cloud was registered through paper targets and consecutive cloud-to-cloud registration. The standard deviation of the registration is 3.67 mm. Finally, the subsampled point cloud with 118 million points was exported as a single file.

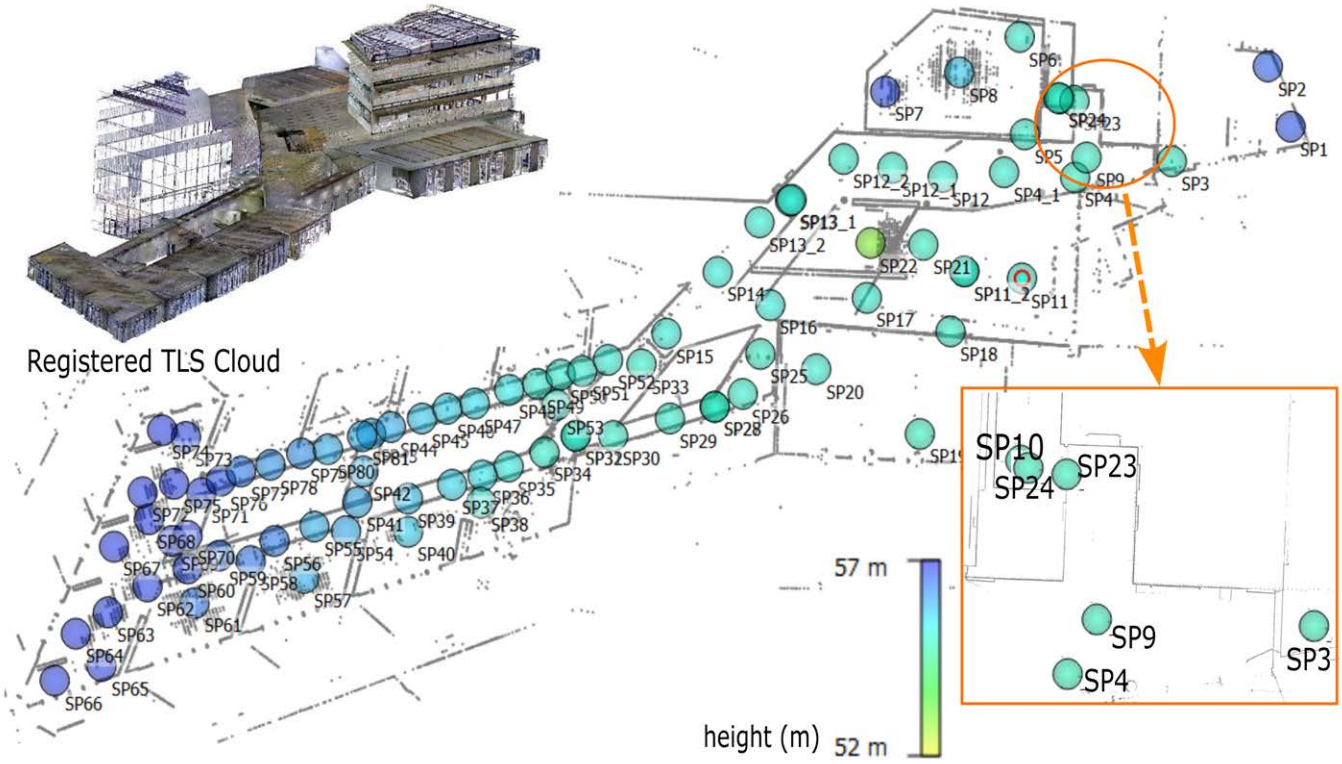

Fig. 4: TLS scan positions during data acquisition including a study area (bottom right) and registered point cloud (top left)

The primary purpose is investigating the NavVis VLX in the context of as-is building documentation for BIM. Therefore, the comparison is focused on the system's performance in the representation of the geometrical characteristics of the test field and the noise in the final point cloud. The comparison methods described below aim to assess how accurate and noise-free representations can be achieved on these objects with NavVis VLX, as these are important factors in building modelling. Before starting the comparison, both systems' point clouds were further cleaned and segmented to have the same coverage. Furthermore, a cloud-to-cloud registration (ICP) was applied via CloudCompare software to eliminate the effect of registration done by different software and people on the datasets. The final root-mean-square (RMS) value of the ICP registration was 8.1 mm.

First, a direct cloud-to-cloud comparison of NavVis VLX and TLS point clouds was done based on the multiscale model-to-model cloud comparison (M3C2) tool in CloudCompare to assess the sensor accuracy. The M3C2 algorithm computes the distances from the core points of a reference cloud to an investigated cloud along the normal vector, which is oriented according to the search surface around the core points (Lague et al. 2013). Then, core points are projected onto the investigated cloud, and computed distances are shown with the colour code.

Next, the contained noise of the point cloud was investigated on the basis of considering particular objects. For this purpose, wall parts from different regions of the floor and columns located in the floor's foyer were chosen as representative objects, which are shown in Fig. 3. Therefore, small parts of various walls covering a 2 to 8 m^2 area from both clouds were segmented, and a best-fit plane was fitted into these segmented clouds. Then, the orthogonal distances from each point to the fitted geometric primitive were measured. The standard deviation of the measurements depicts the deviation from the expected value, represented by the fitted body. Likewise, the best-fit cylinders of the columns located (Fig. 3) were constructed through the RANSAC (**RAN**dom **SA**mpling and **C**onsensus) algorithm, which uses a minimum random set of points and calculates the parameters required to construct the corresponding primitive (Schnabel et al. 2007).

Furthermore, two relatively long (~45–50 m) and narrow (~1.8 m) hallways with gradually sloped floors, the south and north in Fig. 3, were examined. The south hallway is open on one side and has a concrete wall on the other side, while a glass wall borders the north hallway on one side and a concrete wall on the other side. The aim was to evaluate how the NavVis VLX can handle environments with lacking features and sloped grounds. The achievable accuracy in this area is of particular interest. For this assessment, slopes of the south and north hallways were computed on the NavVis VLX data and compared to the values from the TLS data. The values are also cross-checked with the design values from the architectural CAD plans. The slopes were calculated by a plane fitting tool in CloudCompare, which uses the least squares fitting (CloudCompare, n. d.).

4 Comparison of Point Clouds

Fig. 5 shows the M3C2 distances for the first floor with a maximum deviation of 50 mm. Points above this threshold, only around 7 %, were excluded with the assumption of being erogenous errors mostly observed on the reflective and transparent surfaces or around the moved furniture. Within this 50 mm range, the standard deviation is around 9 mm. 91 % of all distances are within the 15 mm range. If the TLS data is considered to represent the actual state, 15 % of the data concerning the presented LOA specifications are in the LOA50 level (0–1 mm), 40 % comply with the LOA40 (1–5 mm), and 36 % is fulfilling the requirements LOA30 (5–15 mm) level.

Another region with a deviation above 20 mm was observed within Area II of Fig. 3. In this case, the operator scanned a nearby control point and returned to it after scanning the narrow and short hallway. Despite the floor and ceiling fitting well, distances between the NavVis VLX and TLS clouds along the wall surfaces exceeded 20 mm. To ensure the reliability of the TLS dataset, some checks were conducted in this area. First check involved verifying the TLS registration for scan positions in this part. According to this, the standard deviation of registration in scan positions SP9, SP4, and SP23 (depicted in Fig. 4) is 1.25, 2.98 and 0.94 mm, respectively, indicating no significant issues. Another check involved comparing the angles between the walls on both sides of the hallway, measured as

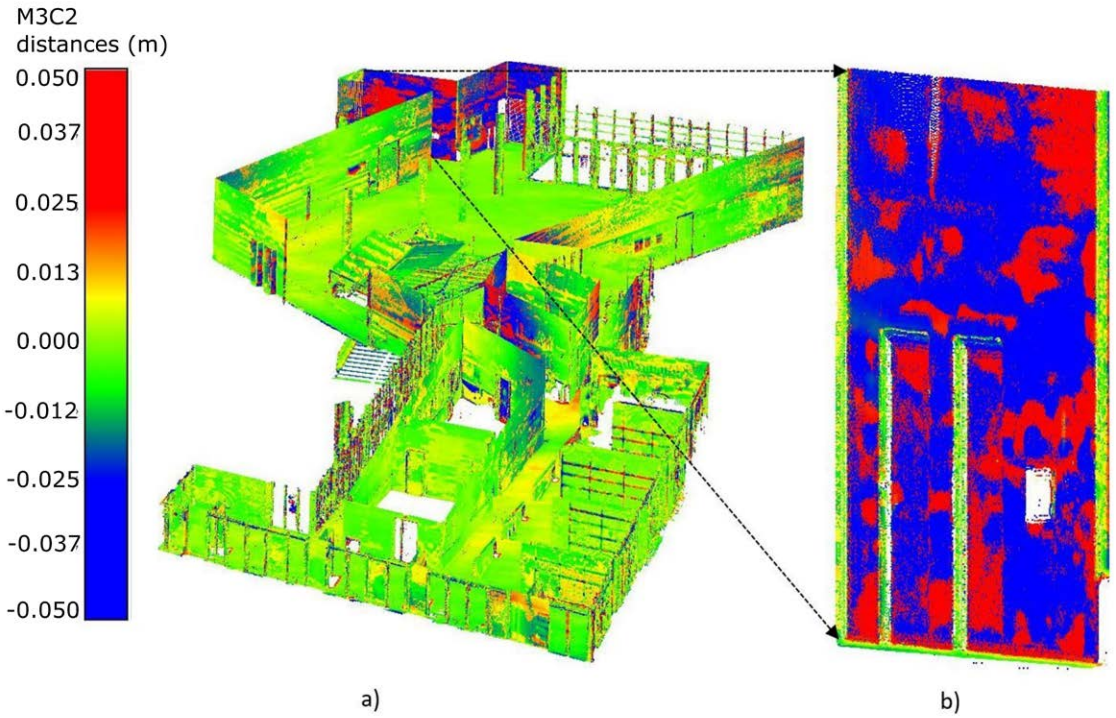

Fig. 5:
a) Cloud-to-cloud comparison of NavVis VLX and TLS.
b) One of the walls with distances exceeding 20 mm is also shown.

The distances between the two clouds are mostly below 20 mm on the floor and the ceiling. However, certain walls exhibit deviations exceeding 20 mm, represented by red and blue colors, such as in Fig. 5(b). Observed deviations in both Area I and II are not uniform; instead, they vary approximately in a range of ±30 mm over the walls' surfaces. One potential reason for this discrepancy is attributed to the missing loop closure of the NavVis VLX. Fig. 3 shows the operator's trajectory based on the stops to take a picture, approximately every 2 m. Notably, there is a missing loop around the marked Area I in Fig. 3, which is a well-known challenge in the SLAM domain. Loop closure is essential to mitigate cumulative errors arising from sensor-based localization (Xiang et al. 2021). Unfortunately, there was no possibility of repeating the scans and proving this argument in this study. However, de Geyter et al. (2022) present how scanning with the loop closure improves the data quality in their work.

Tab. 3: Noise measurements on the concrete wall patches. Dim: dimensions (WxH), PN: the total point number on each patch, and STD: the standard deviation (mm) of the distances to the fitted body

		ZF Imager 5016		NavVis VLX	
	Dim (m^2)	PN	STD (mm)	PN	STD (mm)
Wall1	1.5 x 2.0	55,078	1.3	27,934	1.7
Wall2	3.0 x 2.0	141,279	1.4	63,613	1.8
Wall3	2.0 x 1.0	104,672	0.7	20,936	1.6
Wall4	2.0 x 1.0	61,799	0.7	19,374	1.5
Wall5	4.0 x 2.0	97,887	1.5	28,977	1.7
Wall6	4.0 x 2.0	82,248	1.1	50,129	1.6

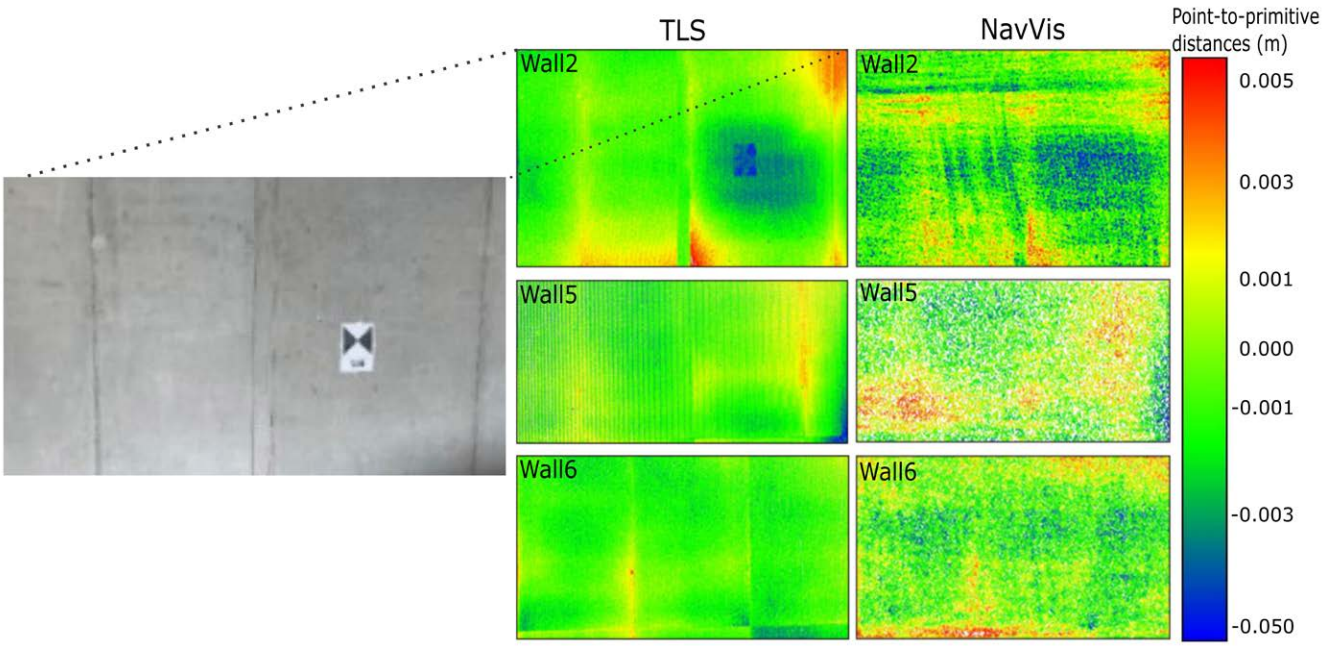

Fig. 6: Noise measurements on Walls 2, 5, and 6. On the left, a picture of Wall 2 is given to show an example of the cracks on the walls, which are obvious on the images.

90° on the available as-designed CAD plans. The angle between the walls on the left side is 90.06° for TLS and 89.89° for NavVis VLX. On the right side, the angle is 89.94° for TLS and 88.80° for NavVis VLX. Based on these measurements, NavVis VLX has bigger deviations than the as-designed values. Thus, a possible reason for the deviation in these areas is considered inaccuracy of the NavVis VLX registration in these parts.

Next, small patches of 2 to 8 m^2 from six different concrete walls, with violet markers in Fig. 3, were cut in both point clouds to assess the noise and point density. The parts were primarily chosen among the plain walls with no wall features. Tab. 3 shows the results, and Fig. 6 depicts the walls 2, 5, and 6 with colour-coded deviations in the range of 5 mm from the fitted planes. The average number of points per square meter for TLS is around 25,000, and about 8,000 points for NavVis VLX. The standard deviation of point distances to the fitted plane is between 1.5 to 1.8 mm for NavVis VLX and changes between 0.7 to 1.5 mm for the TLS. Mainly, higher deviations are observed along the cracks that border concrete blocks or imperfectly flat surface of the concrete wall, which does not have any coating (Fig. 6). Nevertheless, based on these values, it is fair to say that the NavVis VLX can generate point clouds with relatively less noise after its standard post-processing workflow.

A similar assessment was applied to the columns in the first floor's foyer. Again, the best-fit cylinders were constructed, and the point distances to the fitted geometry were calculated to measure the noise. In addition, the point density of each column and the radius of the fitted cylinders compared to the designed value were evaluated. The results are presented in Tab. 4. The average radius measured at columns of the TLS point cloud (R_{TLS}) has a 0.2 mm deviation, which shows that the columns were constructed as designed. The NavVis VLX, on the other hand, depicts columns with a higher point density. It is created by the chosen settings in the post-processing mode.

Tab. 4: Evaluation of columns

	ZF Imager 5016					NavVis VLX			
	Radius (cm)	R_d-R_{TLS} (mm)	Point Number	STD (mm)		Radius (cm)	R_d-R_{VLX} (mm)	Point Number	STD (mm)
Column1	22.40	1.0	39,874	2.7	Column1	22.75	–2.5	50,760	5.2
Column2	22.57	–0.7	50,837	2.4	Column2	22.33	1.7	54,703	5.2
Column3	22.35	1.6	42,953	2.6	Column3	22.02	4.8	58,223	3.8
Column4	22.36	1.4	40,885	1.5	Column4	22.06	4.4	56,942	3.4
Column5	22.71	–2.1	50,622	3.4	Column5	22.44	0.6	43,511	5.8
Average	22.48	0.2	45,034	2.5	Average	22.32	1.8	52,828	4.6

Nevertheless, the average radius measured at columns of the NavVis VLX's point cloud (R_{VLX}) is 22.3 cm, which has a 1.8 mm deviation from the designed radius value (R_d) of 22.5 cm. The standard deviation of the distances from points to the fitted primitives is, on average, 4.6 mm for the NavVis VLX and 2.5 mm for the TLS. Comparing the deviation of the measured radii from the design radius and the average standard deviations of the primitive fitting, it is obvious that both systems have more noise on these curved surfaces in comparison to the planar surfaces (like in Tab. 3). However, the noise in the NavVis VLX point cloud is more prominent. The highest deviation is observed on Column 5, which is located near a glass façade and occluded on the side of this façade. Here, the effect of the occlusion and the reflection on the data can be seen in the results. Overall, looking at the results, an accuracy of around 5 mm is possible with NavVis VLX on curved surfaces like columns.

Furthermore, the behaviour of the NavVis VLX on sloped floors was investigated. The north and south hallways (Fig. 3) have ramps designed with a 6 % slope in parts, and the floor is horizontal (0 % slope) between the ramps. In both point clouds of the TLS and the NavVis VLX, the floor of the hallways was segmented and further divided into eight parts to define each ramp and flat ground separately. For the assessment, a plane was fitted into each part, and the slopes of these planes were compared between the TLS and NavVis VLX and against the designed values.

Tab. 5 summarises the measured slopes and the standard deviation (STD) of the plane fitting. Assuming that the design values represent the actual status, the root-mean-squared error (RMSE) of each slope is calculated and converted into mm. On the ramps of the north hallway, the RMSE is 2.5 mm for the TLS data and 2.7 mm for the NavVis VLX. In comparison, in the south hallway, the RMSE is 0.8 mm and 0.3 mm, respectively.

On the horizontal parts, the RMSE is 1.9 mm for the TLS and 2.9 mm for the NavVis VLX in the north hallway, while it is 1.1 mm for the TLS and 1.5 mm for the NavVis VLX in the south hallway. If the assumption is that the current status of the hallways does not perfectly represent the designed values, and the TLS depicts the best of the actual status, the RMSE of the NavVis VLX would be 0.4 and 0.9 mm for the ramps of north and south hallway, respectively. It would be 1.1 mm for the horizontal parts of the north hallway and 0.6 mm for the south hallway. Overall Tab. 5 shows that the depicted slopes by both systems on the ramps are very similar, on average less than one per thousand, while the difference in slopes of horizontal parts between the two systems is, on average, one per thousand. According to the results, the TLS had the closest representation of the flat surfaces based on the slopes and the standard deviation of the plane fitting. On the ramps, the performance of both systems is similar and higher standard deviations compared to the horizontal parts

Tab. 5: Measured slopes on the fitted planes for the TLS and NavVis VLX planes along with the designed slopes

	TLS		NavVis VLX	
Comparison Area	Slope %	Plane Fitting STD (mm)	Slope %	Plane Fitting STD (mm)
NorthH_Plane1	5.56	5.50	5.56	5.40
NorthH_Plane2	0.16	1.80	0.28	2.20
NorthH_Plane3	6.01	3.10	6.05	2.90
NorthH_Plane4	0.10	2.20	0.19	2.90
NorthH_Plane5	5.99	3.40	5.96	3.70
NorthH_Plane6	0.26	1.90	0.35	2.30
NorthH_Plane7	5.75	3.00	5.70	3.80
NorthH_Plane8	0.21	2.10	0.33	2.50
SouthH_Plane1	6.06	5.80	5.99	5.80
SouthH_Plane2	0.07	1.40	0.16	2.40
SouthH_Plane3	5.91	4.00	5.98	4.30
SouthH_Plane4	0.16	1.90	0.14	2.30
SouthH_Plane5	5.99	2.60	5.99	2.70
SouthH_Plane6	0.07	1.60	0.16	2.60
SouthH_Plane7	5.89	1.40	6.05	2.70
SouthH_Plane8	0.12	1.60	0.16	2.40

Fig. 7: A small section of the stairs connecting first floor to the ground floor, captured by the TLS (top) and NavVis VLX (bottom)

might be a possible result of the wearing in time on the sloped ground.

Lastly, the representation of stairs in the point cloud is compared. Fig. 7 depicts the upper part of the stairs connecting the first floor to the ground floor. It is difficult to capture each step with a TLS, as it needs multiple setups, which does not always offer the full view. In this work, the instrument was set up on top, bottom and middle of the stairs and could not capture all steps completely. On the contrary, the NavVis VLX captured the whole steps while walking in one direction. For that reason, the real situation can be modelled based on the point cloud itself. Nevertheless, it is seen that the TLS depicts sharper edges in the captured steps, whereas NavVis VLX's cloud struggles to represent these sharp edges. However, the NavVis VLX data resolution was set to 10 mm during post-processing, which subsamples the data, and the sharpness might be increased if the resolution is set to a higher value.

5 Discussion and Conclusion

This paper evaluates the performance of the NavVis VLX in comparison to a terrestrial laser scanner in indoor scenarios, especially in the AEC domain. Evaluation is focussed on the accuracy of the generated point cloud through a direct comparison to the reference dataset and the device noise through the primitive fitting. Based on the cloud-to-cloud comparisons, NavVis VLX demonstrated a good performance, where only 2 % of deviations are higher than 25 mm compared to a reference point cloud. This also shows that the reached accuracy lies around 25 mm as opposed to the relative accuracy of 8 mm (Tab. 2) demonstrated by NavVis. Campi et al. (2022) also present a similar result in a cloud-to-cloud comparison of NavVis VLX and a TLS reference dataset. While the floor and ceiling fit well, higher deviations can be seen on the wall surfaces, possibly resulting from the trajectory errors in the SLAM algorithm due to the missing loop closures, which is a known problem for SLAM sensors (Burgard et al. 2010).

In terms of noise, NavVis VLX delivers a relatively clean point cloud (after standard post-processing of the data) with a compatible standard deviation to the TLS data. However, sharp edges are not as precise as the TLS data, as seen on the steps of the stairs. Nevertheless, capturing whole stairs with only one way of walking is possible, which is pretty handy for modelling tasks. The NavVis VLX produced clean point clouds on curved surfaces like columns, but it did not overtake the TLS in fitting accurate geometries.

The results prove that the NavVis VLX is a compatible mobile mapping system for many applications in the AEC domain, especially in building modelling (Scan2BIM). According to the LOA specifications depicted in Tab. 1, the demonstrated accuracy complies with the measurement accuracies of LOA 20 and 30.

Besides the accuracy, a noise-free point cloud is of utmost importance for accurate and fast modelling. In this regard, the NavVis VLX offers a satisfying product. Only the post-processed NavVis VLX data is used in this assessment. Hence, the results are interpreted as the fine work of NavVis' post-processing workflow, and it is fair to say that the post-processing algorithm of NavVis VLX works quite fine and also detects and cleans the noise caused by glass windows. On the other hand, missing sharpness around the edges can be a disadvantage for very detailed modelling works like it is required for LOA40 or LOA50.

In addition to the modelling aspect, the time spent on data collection and labour are the other critical criteria in industry. Here, mobile systems have a clear advantage over the TLS. As in this paper's example, the whole floor was scanned by one operator in two days with the TLS, including placing the targets. In contrast, the data capture for the same area took only around one hour of work by one operator with the NavVis VLX.

Acknowledgement

This paper was written within the L5IN project, funded by the Federal Ministry of Transport and Digital Infrastructure (BMVI) grant number VB5GFHAMB.

The authors thank DiConneX GmbH for supporting this work by providing the NavVis VLX data, the data acquisition and processing.

It is an independent work and has no support from NavVis GmbH.

References

Becker, R., Clemen, C., Wunderlich, T. (2022): BIM in der Ingenieurvermessung. In: DVW e. V. und Runder Tisch GIS e. V. (Hrsg): Leitfaden Geodäsie und BIM. Version 3.1. Bühl/München, 83–95.

Borrmann, A., König, M., Koch, C., Beetz, J. (2018): Building Information Modeling: Why? What? How? In: Building Information Modeling: Technology Foundations and Industry Practice, 1–24. Springer International Publishing. DOI: 10.1007/978-3-319-92862-3_1.

Burgard, W., Stachniss, C., Arras, K., Bennewitz, M. (2010): SLAM: Simultaneous Localization and Mapping. In: Introduction to Mobile Robotics. [Lecture notes]. http://ais.informatik.uni-freiburg.de/teaching/ss11/robotics/slides/12-slam.pdf, last access 01/2023.

Campi, M., Falcone, M., Sabbatini, S. (2022): Towards Continuous Monitoring of Architecture. Terrestrial Laser Scanning and Mobile Mapping System for the Diagnostic Phases of the Cultural Heritage. International Archives of the Photogrammetry, Remote Sensing and Spatial Information Sciences – ISPRS Archives, 46(2/W1-2022), 121–127. DOI: 10.5194/ISPRS-ARCHIVES-XLVI-2-W1-2022-121-2022.

CloudCompare (n. d.): Fit Plane – CloudCompareWiki. www.cloudcompare.org/doc/wiki/index.php/Fit_Plane, last access 03/2023.

de Geyter, S., Vermandere, J., de Winter, H., Bassier, M., Vergauwen, M. (2022): Point Cloud Validation: On the Impact of Laser Scanning Technologies on the Semantic Segmentation for BIM Modeling and Evaluation. Remote Sensing, 14(3). DOI: 10.3390/rs14030582.

DIN (2010): DIN 18710-1:2010-09, Ingenieurvermessung – Teil 1: Allgemeine Anforderungen.

Heinz, E., Eling, C., Klingbeil, L., Kuhlmann, H. (2020): On the applicability of a scan-based mobile mapping system for monitoring the planarity and subsidence of road surfaces-Pilot study on the A44n motorway in Germany. Journal of Applied Geodesy, 14(1), 39–54. DOI: 10.1515/jag-2019-0016.

Higgins, S. (2020a): How SLAM affects the accuracy of your scan (and how to improve it). www.navvis.com/blog/how-slam-affects-the-accuracy-of-your-scan-and-how-to-improve-it.

Higgins, S. (2020b): Designing NavVis VLX: wearable mobile mapping for day-to-day surveying. www.navvis.com/blog/designing-navvis-vlx-wearable-mobile-mapping-for-day-to-day-surveying.

Janßen, J., Kuhlmann, H., Holst, C. (2022): Target-based terrestrial laser scan registration extended by target orientation. Journal of Applied Geodesy, 16(2), 91–106. DOI: 10.1515/jag-2020-0030.

Keller, F. (2016): Entwicklung eines forschungsorientierten Multi-Sensor-Systems zum kinematischen Laserscanning innerhalb von Gebäuden. Dissertation, HafenCity Universität Hamburg. https://d-nb.info/1095495798/04.

Lague, D., Brodu, N., Leroux, J. (2013): Accurate 3D comparison of complex topography with terrestrial laser scanner: application to the Rangitikei canyon (N-Z). ISPRS Journal of Photogrammetry and Remote Sensing, 82, 10–26. DOI: 10.1016/j.isprsjprs.2013.04.009.

Lehtola, V. V., Kaartinen, H., Nüchter, A., Kaijaluoto, R., Kukko, A., Litkey, P., Honkavaara, E., Rosnell, T., Vaaja, M. T., Virtanen, J. P., Kurkela, M., El Issaoui, A., Zhu, L., Jaakkola, A., Hyyppä, J. (2017): Comparison of the selected state-of-the-art 3D indoor scanning and point cloud generation methods. Remote Sensing, 9(8). DOI: 10.3390/rs9080796.

Lehtola, V. V., Nikoohemat, S., Nüchter, A. (2021): Indoor 3D: Overview on Scanning and Reconstruction Methods. In: Werner, M., Chiang, Y.-Y. (Eds.): Handbook of Big Geospatial Data. Springer. 55–97. DOI: 10.1007/978-3-030-55462-0_3.

Maboudi, M., Bánhidi, D., Gerke, M. (2017): Evaluation of indoor mobile mapping systems. GFal Workshop 3D-NordOst, Berlin, Germany, 7-8 December. 125–134.

NavVis (2020): NavVis VLX Fast capture for AEC. NavVis. [Productt Information].

NavVis. (2023): The NavVis Blog | Powered by NavVis. www.navvis.com/blog/tag/powered-by-navvis, last access 04/2023.

Otero, R., Lagüela, S., Garrido, I., Arias, P. (2020): Mobile indoor mapping technologies: A review. Automation in Construction, 120, 103399. DOI: 10.1016/j.autcon.2020.103399.

Prokhorov, D., Zhukov, D., Barinova, O., Vorontsova, A., Konushin, A. (2019): Measuring robustness of Visual SLAM. 16th International Conference on Machine Vision Applications (MVA), 1–6. DOI: 10.23919/MVA.2019.8758020.

Salgues, H., Macher, H., Landes, T. (2020): Evaluation of Mobile mapping Systems for Indoor Surveys. The International Archives of the Photogrammetry, Remote Sensing and Spatial Information Sciences, XLIV-4/W1-(4/W1), 119–125. DOI: 10.5194/isprs-archives-XLIV-4-W1-2020-119-2020.

Schnabel, R., Wahl, R., Klein, R. (2007): Efficient RANSAC for Point-Cloud Shape Detection. Computer Graphics Forum, 26(2), 214–226. DOI: 10.1111/j.1467-8659.2007.01016.x.

Schuldt, C., Shoushtari, H., Hellweg, N., Sternberg, H. (2021): L5IN: Overview of an Indoor Navigation Pilot Project. DOI: 10.3390/rs13040624.

Soudarissanane, S. (2016): The Geometry of Terrestrial Laser Scanning: Identification of Errors, Modelling and Mitigation of Scanning Geometry. Dissertation, Technische Universität Delft. https://repository.tudelft.nl/islandora/object/uuid%3Ab7ae0bd3-23b8-4a8a-9b7d-5e494ebb54e5.

Tucci, G., Visintini, D., Bonora, V., Parisi, E. I. (2018): Examination of indoor mobile mapping systems in a diversified internal/external test field. Applied Sciences (Switzerland), 8(3). DOI: 10.3390/app8030401.

U. S. Institute of Building Documentation (2016): USIBD Level of Accuracy (LOA) Specification Guide, v2.0-2016. Technical report.

Wang, Q., Guo, J., Kim, M. K. (2019): An application oriented scan-to-bim framework. Remote Sensing, 11(3). DOI: 10.3390/rs11030365.

Wu, C., Yuan, Y., Tang, Y., Tian, B. (2022): Application of terrestrial laser scanning (TLS) in the architecture, engineering and construction (AEC) industry. Sensors, 22(1). DOI: 10.3390/s22010265.

Xiang, H., Shi, W., Fan, W., Chen, P., Bao, S., Nie, M. (2021): FastLCD: A fast and compact loop closure detection approach using 3D point cloud for indoor mobile mapping. International Journal of Applied Earth Observation and Geoinformation, 102, 102430. DOI: 10.1016/J.JAG.2021.102430.

Zoller + Fröhlich. (n. d.): Z+F IMAGER® 5016: Zoller+Fröhlich. www.zofre.de/en/laser-scanners/3d-laser-scanner/z-f-imagerr-5016, last access 07/2022.

Contact
Cigdem Askar
Landesbetrieb Geoinformation und Vermessung
Neuenfelder Straße 19, 21109 Hamburg
cigdem.askar@gv.hamburg.de

Annette Scheider | Harald Sternberg
HafenCity Universität Hamburg
Professur für Hydrographie und Geodäsie
Henning-Voscherau-Platz 1, 20457 Hamburg
annette.scheider@hcu-hamburg.de
harald.sternberg@hcu-hamburg.de

This article also is digitally available under www.geodaesie.info.